

# Information embedding in electrophotographic document forms through laser intensity modulation – a communications systems perspective

Maria V. Ortiz Segovia, George T.-C. Chiur†, Edward J. Delp, and Jan P. Allebach; School of Electrical and Computer Engineering, †School of Mechanical Engineering, Purdue University; West Lafayette, Indiana/United States

## Abstract

*Printed documents have been used as accessories to fraud, terrorist attacks, forgery, and extortion. Tracking down the printer that was used to produce such documents may be beneficial to law enforcement and military agents. Printer identification requires the extraction of a set of features or signatures that uniquely represent the printer. These signatures can be inherent or intrinsic to the printing process, or they can be artificially produced and embedded during the printing process. In this paper, the hidden information for an electrophotographic (EP) printer is generated by altering the laser beam intensity from scan line to scan line, which results in dot gain, and shift in the horizontal position of the dots. Techniques from digital communications are applied to this embedding signal to make it imperceptible, but reliably transmitted and recovered. The embedding signal is inserted in the frames or borders of security documents such as bank notes, statements, and event tickets. Such an embedding scheme offers a content-independent domain for marking the print compared to using text characters or halftone images.*

## Introduction

Printed documents of any kind (text, images, bank statements, boarding passes, event tickets, etc) have been used as means of fraud, terrorist attacks, forgery, and threatening notes, among other crimes. It is highly relevant for forensic analysis to identify the technology, brand, and serial number of the printer that was used to print a fraudulent document. Among several methods for document security, embedding imperceptible information in a printed document can be used as an instrument for printer identification, authentication of document content, and proof of ownership.

A considerable amount of forensic information is contained in printed documents. Most of this forensic information is caused by inherent defects of the physical components of the printer. In order to recover and link the forensic traces from a document to a particular printer brand and model, a prior understanding and modeling of the device mechanism is required. An alternative approach can be taken for document security. Rather than using the inherent or intrinsic signatures of the printer, we can artificially generate and insert imperceptible information in the document to tie it to the printer that originated it. The artificial or extrinsic information can be embedded in the document at any stage of the printing pipeline by either altering the document before it is sent to the printer, or by modifying process parameters in the printer mechanism as the document is printed. We believe that moving the embedding step into the printer hardware makes the signature

less susceptible to tampering compared to watermarking the digital version of the document. The signature can be designed to carry information such as a time stamp, the printer serial number, or a secure hash of the document content.

One of our previously developed methods embeds information at the printer mechanism level through amplitude modulation of the laser beam intensity (LBI) [1]. Modulation of the LBI allows per-scan-line changes in dot size and position. A set of sinusoids of different frequencies and amplitudes can be used to embed information in halftone images and text characters. In halftone images, the embedded signal can be easily recovered through frequency analysis of large mid-tone gray patches [2]. But the regions of the image with gray values that fall on the extreme levels of the gray scale, such as highlight and black patches, are not useful for detecting the embedded signal due to their toner concentrations. Also, the synchronization of the signal among the portions of the image that are suitable for embedding becomes a challenge.

For dark solid regions, such as text characters, another detection approach needs to be taken [3]. In text documents, the straight edges of text characters can be extracted to recover the extrinsic signature. In fact, the vertical edge profile is ideally similar to the signature carrier waveform. The reported embedding capacities in halftone images and text characters are around 20-30 bits per inch and 200-400 bits per page respectively.

When neither text characters nor large mid-tone gray areas are present, the strategies mentioned above cannot be implemented. In this paper we propose to use elements of *forms*, such as borders, to embed signatures. Typical security documents such as bank notes, statements, and event tickets usually contain a frame or border around the edge of the document that can carry the embedded information. This embedding scheme offers a wider content-independent domain for marking the print compared to using text characters or halftone images.

Signal detection methods similar to those used for text characters can be adapted for forms, but since a frame is usually much longer than a text character and is continuous, a wider range of embedding approaches can be explored. The length and continuity of borders facilitate the implementation of error-correcting coding techniques that are not practical to apply on text characters, or halftone images with small and scattered mid-tone gray areas.

In the following sections of the paper, we discuss the extrinsic signature embedding and recovery strategies for document borders. We will also present the encoding and decoding methods that are implemented for the embedded signal along with our

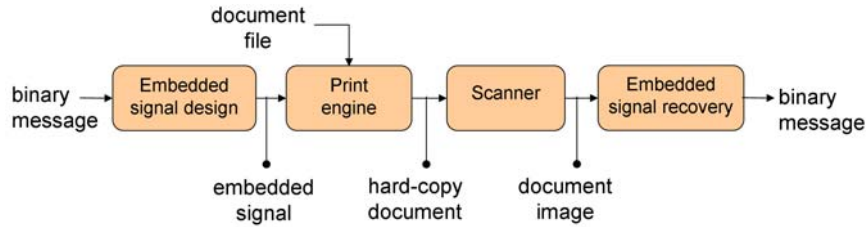


**Figure 1.** Block diagram for extrinsic signature embedding. The embedded signal is designed based on the binary message. Then, the signature is printed and scanned as part of the document. Finally, the image of the document is analyzed and the message is recovered.

experimental results and conclusions.

## A communications systems perspective

Our signature embedding scheme can be seen as a communications system, where the message to be transmitted is the extrinsic signature, and the communications channel is the border or frame in the document. The information carrier is composed of a sequence consisting of waveform segments drawn from two distinct code words, one for each bit of the binary message. The transmission noise is mostly generated by the instabilities of the electrophotographic (EP) printing technology.

As mentioned above, the length and continuity of borders allow us to explore coding methods from the area of communications with error-correcting capabilities, which result in a higher embedding capacity and a more reliable embedding method. We chose two error-correcting codes that exhibit attributes from different coding categories: Reed-Solomon (RS) codes [4] and convolutional codes (CC) [4]. The RS code that we implemented is systematic and uses a hard-decision decoder. In contrast, the CC code is non-systematic and employs a soft-decision decoder. A code is said to be systematic if the encoded message contains the information bits unchanged with some parity bits added. Similarly, a non-systematic code is one in which the output does not contain the input bits.

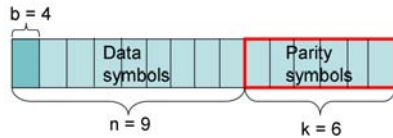


**Figure 2.** Message structure for an RS (15,9) encoder. The RS encoder encodes 9-data-symbol blocks at a time, and returns blocks of 15 symbols. The 6 parity symbols provide an error-correcting capacity of 3 symbol errors. Each symbol is composed of 4 bits.

The chosen RS processes data in segments of 36 bits that are organized in groups of 4 bits each called symbols, to which a sequence of 24 parity bits is added. The parity bits are also organized into groups of 4-bit symbols. The result is a block of 60 bits or 15 symbols that is processed as a unit by the encoder/decoder pair. The decoder can correctly decode the data symbols, even if up to 3 symbols are in error anywhere in the block. For a symbol that is in error, errors can be located in any or all of the bits that comprise that symbol. The code rate of the RS encoder is  $36/60 = 0.6$ . For decoding, we follow the traditional approach specified by the Berlekamp-Massey, Chien search, and Forney algorithms [4]. The RS encoded message structure is displayed in Fig. 2.

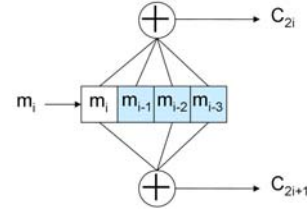


**Figure 3.** Encoder (2,4,1) for the convolutional code. Each bit  $m_i$  of the original message is encoded by 2 bits,  $c_{2i}$  and  $c_{2i+1}$ . The encoded message is twice as long as the original one. Note that the two outputs  $c_{2i}$  and  $c_{2i+1}$  differ only in that for  $c_{2i+1}$ , the input  $m_{i-1}$  is excluded from the logical OR.

On the other hand, our implementation of the CC method employs the (2,4,1) encoder of Fig. 3. The encoder has a code rate of  $1/2 = 0.5$  which produces an encoded message that is twice as long as the original one. The error-correcting capacity for CC depends on the free distance  $d_{free}$  of the code, which is the minimum Hamming distance between any two distinct code sequences. A CC can correct any error pattern of up to  $t$  errors, where  $2t < d_{free}$  [6]. Our CC has a free distance of 6. The received message is decoded by an Euclidean metric based Viterbi decoder [5].

## Extrinsic signature embedding and recovery

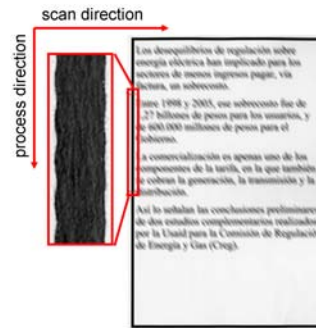


**Figure 4.** Sample of sinusoidal signal embedded in the border of a document. The effects of dot gain and dot shifting due to amplitude modulation of the laser beam intensity are observed on the edges of the border. For purposes of illustration, the modulation is much larger than it would be in practice.

The block diagram of Fig. 1 describes the signature embedding and recovery process. First, the message carrier (or embedded signal) is designed according to the encoded binary message and is inserted in the document during the printing stage. The

printout is later scanned with a flatbed scanner at 600 dpi. Subsequently, the form or border is segmented out from the document image. Finally, the embedded signal is extracted from the edge profile and decoded to recover the binary message.

The EP printing process stages of exposure and development are perturbed by the insertion of the signature. In the exposure stage, specific locations of the organic photoconductor (OPC) drum surface are discharged by a laser beam. During the stage of development, the discharged regions attract toner particles from the developer roller. This image is later transferred and fused to the paper.

The intensity of the laser beam that discharges the OPC surface is proportional to the voltage that feeds the laser beam assembly. The embedding signal modulates the amplitude of the voltage, which results in the modulation of the LBI. The voltage is changed from scan line to scan line. Therefore, the signature affects only the content of the printout in the direction in which the paper moves through the printer referred to as the *process direction*, as illustrated in Fig. 4.

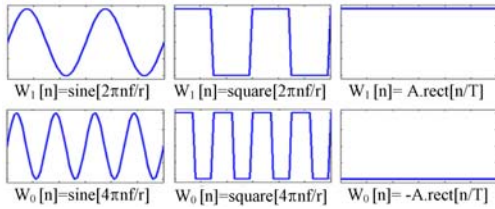


**Figure 5.** Code word choices ( $n = 0, 1, \dots, T$  and  $r = 600 \text{ dpi}$ ). The first row shows the options for the bit '1'; and the second one shows the choices for the bit '0'. The x-axis represents the scan line index and the y-axis is the code word amplitude. In the plots for sine and square waves, we show 2 and 4 cycles of the lower and higher frequency signals, respectively. For the constant amplitude waveform, the number of scan lines per code word determines the support or domain of the function.

### Embedded signal design

The modulating signal is designed in the first stage of the block diagram of Fig. 1. Different signal attributes, including the waveform of the carrier, are adjusted or chosen within this block. Even though different values of amplitude, frequency (in cycles per inch) and code word length (in scan lines) can be considered, the set of options is constrained by the physical limitations of the printer, the instabilities of the EP process, and the perceived raggedness at the edges of the lines in the form.

The limitation on the embedding signal amplitude is set by the raggedness values of the edges of the borders. The ideal vertical contour that is used to measure raggedness, as defined by [7], is presented in (1), where  $R_{max}$  is the maximum reflectance of the substrate and  $R_{min}$  is the minimum reflectance of the colorant.

$$R_{60} = R_{max} - \frac{60}{100}(R_{max} - R_{min}). \quad (1)$$

Sine, square, and constant amplitude waveforms are the options that were tested for signature carriers. The code words for a sine or a square wave carrier are defined by a pair of frequencies, where the lower frequency represents the bit '1' and the higher frequency the bit '0'. For the constant amplitude waveform, two

opposite amplitudes are used as code words, the negative value for the bit '0' and the positive value for the bit '1'. A summary of the code word alternatives is presented in Fig. 5.

The signature carrier  $S[y]$  is shown in (2), where  $T$  is the length of each code word in scan lines,  $A$  is the embedding signal amplitude, and  $V_o$  is the bias voltage of the laser beam unit. The signal depends on  $y$ , which is the scan line index. The length in bits of the encoded message is  $L$ . The encoded bits  $c_i$  0 or 1 determine which code word segment,  $W_0$  or  $W_1$ , is to be used in the embedded signal for the  $i$ -th code word.

$$S[y] = \sum_{i=0}^L A \cdot W_{c_i}[y - iT] + V_o. \quad (2)$$

### Embedded signal recovery

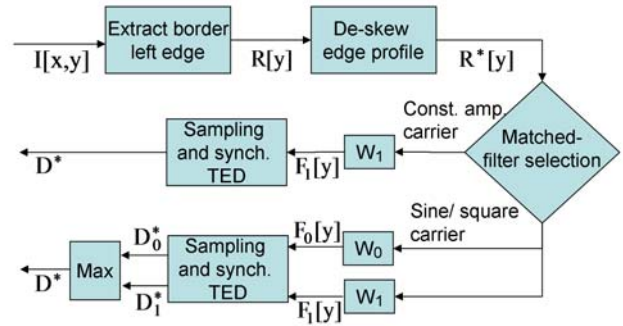


**Figure 6.** Block diagram for the embedded signal recovery process. In the matched-filtering stage one of two different paths is to be taken depending on the waveform of the embedded signal.

The signal recovery starts after the printout is scanned and the border of the form is segmented from the scanned image. The recovery process is illustrated in the block diagram of Fig. 6. First, we use (3) to extract the left edge  $R[y]$  of the border, where  $I[x,y]$  is the grayscale image of the form and  $R_{60}$  is the threshold set by (1). The right edge of the border can be extracted by finding the maximum value of the set in (3) instead of the minimum.

$$R[y] = \min(\{x | I[x,y] > R_{60}\}). \quad (3)$$

Then,  $R[y]$  is de-skewed by a linear least squares method to correct for the skew error that occurred during scanning. Subsequently, the de-skewed 1-D edge profile is passed through a set of matched-filtering operators to get  $F_j[y]$ , as seen in (4), where  $R^*[y]$  is the de-skewed edge profile and the symbol  $\otimes$  indicates convolution. For the sine and square wave carriers, we employ two matched-filters which correspond to the low and high frequency signals for each carrier. In the case of the constant amplitude carrier, only one matched-filter is used. Two different paths leave the matched-filter selection block in Fig. 6, one corresponding to the constant amplitude carrier and the other corresponding to the sine or square wave carriers.

$$F_j[y] = R^*[y] \otimes W_j[-y], \quad j = \begin{cases} 0, 1, & \text{square/sine wave carrier,} \\ 1, & \text{constant amplitude carrier.} \end{cases} \quad (4)$$

The matched-filtering output flags the positions of the code words through the peaks in the correlation between the signal and the filter. The correlation peaks are ideally located in multiples of the code word length  $T$ . To address sampling synchronization issues due to noise, a timing error detector (TED) is also included in the signal recovery process [8]. The TED looks for the local maximum within  $\tau/2$  samples before and after the ideal sampling time  $mT$  in  $F_j[y]$ , as seen in (5).

$$D_j^*[m] = \max\{F_j[y] ; mT - \tau/2 \leq y \leq mT + \tau/2\}. \quad (5)$$

For the constant amplitude carrier, the samples in  $D_1^*[m]$  are ready to be sent to the decoder to recover the original message, i.e.  $D_1^*[m] = D^*[m]$ . On the other hand, when the embedded signal is a sine or square wave, another step prior to decoding is required. We need to compare the outputs of the synchronization step and pick the largest sample to determine whether the symbol  $W_o[n]$  or  $W_1[n]$  was transmitted. We describe this last step in (6).

$$D^*[m] = \max(D_o^*[m], D_1^*[m]). \quad (6)$$

## Experimental setting and results

The complete embedding system was tested with several combinations of code word parameters and coding schemes. The printing and scanning resolution is 600 dpi. We used an HP Color LaserJet 4500 printer, and an Epson Expression 10000XL scanner. The laser beam assembly of the printer had been altered to grant access to the LBI mechanism. Although a color printer is used as the experimental platform, we will only focus on the monochrome results.

The set of frequency pairs for the sine and square waveforms is  $\{(20,40), (30,60), (50,100)\}$ . The code word length depends on the number of cycles that are used per code word. In particular, we used one cycle of the lower frequency and two cycles of the higher frequency of the pairs (20,40), (30,60), and three and six cycles of the lower and higher frequency of the pair (50,100), respectively. For the constant amplitude carrier, code word lengths of between six and ten scan lines were tested.

The RS (15,9) encoder takes 9-symbol blocks of the original message and encodes them into 15-symbol blocks. For the CC, we employed an original message of 7 bits, which gives an encoded message of 14 bits. In a Trellis diagram,  $d_{free}$  can be calculated by comparing every path with the all-zero path [6]. The implemented CC has a free distance of 6.

The results presented in Table 1 show that when the message is not encoded, the embedding capacity is similar to the capacities reported for halftone images and text characters. In contrast, the capacity increases substantially when the coding techniques presented here are included.

## Conclusions

We have proposed a reliable data embedding and recovery scheme for elements in document forms, such as borders, by amplitude modulation of the laser beam intensity. The use of the edges of the borders as signature carriers provides the opportunity to increase the embedding capacity significantly through coding strategies that have error-correcting capabilities. Document forms

**Table 1: Embedding capacity and error rates for encoded signature carriers. The units are scan lines.**

Code	Carrier	Symb. or bit length	Code word length	Capacity bits/inch	Error rate
-	sine (20,40)	30	30	20	2.3%
-	sine (50,100)	12	36	16	3%
-	square (20,40)	30	30	20	0%
-	square (50,100)	12	36	16	0%
RS	constant	7	28	85	4.8%
RS	constant	8	32	75	0%
CC	constant	7	14	85	3.1%
CC	constant	8	16	75	0%

offer a wider domain for embedding signatures than text characters and halftone images.

## References

- [1] P.-J. Chiang, G. N. Ali, A. K. Mikkilineni, G. T.-C. Chiu, J. P. Allebach, E. J. Delp, "Extrinsic signatures embedding using exposure modulation for information hiding and secure printing in electrophotographic devices," in Proc. IS&T's NIP20: International Conference on Digital Printing Technologies, vol. 20, 2004, pp. 295-300.
- [2] P.-J. Chiang, A. K. Mikkilineni, O. Arslan, R. M. Kumontoy, G. T.-C. Chiu, E. J. Delp, J. P. Allebach, "Extrinsic Signatures Embedding and Detection in Electrophotographic Halftone Images through Laser Intensity Modulation", in Proc. IS&T's NIP22: International Conference on Digital Printing Technologies, vol. 22, 2006, pp. 432-435.
- [3] A. K. Mikkilineni, P.-J. Chiang, S. Suh, G. T.-C. Chiu, J. P. Allebach, E. J. Delp, "Information embedding and extraction for electrophotographic printing processes," in Proc. SPIE International Conference on Security, Steganography, and Watermarking of Multimedia Contents VIII, vol. 6072, 2006.
- [4] P. Sweeney, Error Control Coding: From Theory to Practice, Wiley, New York, NY, 2002.
- [5] S. Haykin, Communication Systems, Wiley, New York, NY, 2001.
- [6] R. Blahut, Algebraic Codes for Data Transmission, Cambridge University Press, 2003.
- [7] ISO/IEC DIS 13660, "Office Equipment - Measurement of image quality attributes for hardcopy output - Binary monochrome text and graphic images," International Organization for Standardization, 2001.
- [8] L. Litwin, (2001, September). Matched filtering and timing recovery in digital receivers. [Online]. Available: <http://www.rfdesign.com>.

## Author Biography

*Maria V. Ortiz Segovia received her B.S. degree from the Universidad Javeriana, Bogota, Colombia, in 2005. She is currently pursuing her Ph.D. degree in electrical and computer engineering at Purdue University. Her current research interests include image processing, color imaging, and printer forensics.*